



HHS PUBLIC ACCESS

Author manuscript

Clin Genet. Author manuscript; available in PMC 2017 October 01.

Published in final edited form as:

Clin Genet. 2016 October ; 90(4): 351–360. doi:10.1111/cge.12739.

Disrupted Nitric Oxide Signaling due to *GUCY1A3* Mutations Increases Risk for Moyamoya Disease, Achalasia and Hypertension

Stephanie Wallace¹, Dong-chuan Guo¹, Ellen Regalado¹, Lauren Mellor-Crummey¹, Michael Banshad², Deborah A. Nickerson², Robert Dauser³, Neil Hanchard⁴, Ronit Marom⁴, Emil Martin¹, Vladimir Berka¹, Iraida Sharina¹, Vijeya Ganesan⁵, Dawn Saunders⁶, Shaine Morris⁷, and Dianna M. Milewicz, MD¹

¹Division of Medical Genetics, Cardiology, and Hematology, Department of Internal Medicine, University of Texas Health Science Center, Houston, Texas

²Department of Genome Sciences, University of Washington, Seattle, Washington

³Department of Neurosurgery, Texas Children's Hospital, Houston, Texas

⁴Department of Molecular and Human Genetics, Baylor College of Medicine, Houston, Texas

⁵Neuroscience Unit, University College of London Institute of Child Health, London, UK

⁶Department of Radiology, Great Ormond Street Hospital, London, UK

⁷Department of Pediatrics – Cardiology, Texas Children's Hospital and Baylor College of Medicine, Houston, Texas

Abstract

Moyamoya disease (MMD) is a progressive vasculopathy characterized by occlusion of the terminal portion of the internal carotid arteries and its branches, and the formation of compensatory moyamoya collateral vessels. Homozygous mutations in *GUCY1A3* have been reported as a cause of MMD and achalasia.

Probands (n = 96) from unrelated families underwent sequencing of *GUCY1A3*. Functional studies were performed to confirm the pathogenicity of identified *GUCY1A3* variants.

Two affected individuals from unrelated families were found to have compound heterozygous mutations in *GUCY1A3*. MM041 was diagnosed with achalasia at 4 years of age, hypertension and MMD at 18 years of age. MM149 was diagnosed with MMD and hypertension at the age of 20 months. Both individuals carry one allele that is predicted to lead to haploinsufficiency and a second allele that is predicted to produce a mutated protein. Biochemical studies of one of these alleles, *GUCY1A3*Cys517Tyr, showed that the mutant protein (a subunit of soluble guanylate cyclase) has a significantly blunted signaling response with exposure to nitric oxide.

Correspondence: Dianna M. Milewicz, M.D., Ph.D., Department of Internal Medicine, MSB 6.100, 6431 Fannin Street, Houston, Texas 77030. Dianna.M.Milewicz@uth.tmc.edu. Phone: 713-500-6715 Fax: 713-500-0693.

Conflict of Interest Statement: The authors declare no conflict of interest.

GUCY1A3 missense and haploinsufficiency mutations disrupt nitric oxide signaling leading to MMD and hypertension, with or without achalasia.

Keywords

stroke; moyamoya disease; achalasia; *GUCY1A3*; genetic; rare variants

INTRODUCTION

Moyamoya disease (MMD) is a cerebrovascular disease characterized by progressive stenosis of the terminal portion of the internal carotid arteries and its branches, leading to compensatory neovascularization and the moyamoya, or “puff of smoke”, appearance of these vessels on angiogram (1). Individuals with MMD may present with ischemic strokes, intracerebral hemorrhage or transient ischemic attacks. The condition has two peaks in the age of onset of symptoms, the first in childhood and a second peak in the 4–5th decade of life. Neurosurgical intervention to prevent further strokes in these patients is available; however, preventing or reversing the occlusion of the distal internal carotid arteries through medical management is currently not available.

Several genetic conditions predispose to MMD, including Down syndrome, Alagille syndrome, neurofibromatosis type 1 (NF1), and sickle cell disease (2–4). MMD can also be associated with short stature, hypergonadotropic hypogonadism and facial dysmorphism due to deletion of *BRCC3* and *MTCP/MTCP1NB* on the X chromosome (5). MMD can be inherited in families in the absence of a known syndrome in an autosomal dominant inheritance pattern with decreased penetrance in the absence of syndromic features (6, 7). A number of genes have been identified for MMD not associated with a syndrome. A subset of missense mutations in *ACTA2* lead to bilateral stenosis or occlusion of the distal internal carotid artery, with some similarities to MMD, but these patients do form the compensatory collateral vessels and often have characteristically straight arteries as well as dilated more proximal carotid vessels. Thus, cases due to *ACTA2* mutations are classified as having MMD-like cerebrovascular pathology (8, 9). Additionally, a founder variant, p.R4810K, is associated with MMD in Asian patients and segregates with disease in Asian families, which may be the basis for the increased frequency of MMD in Japan (10, 11). Although *RNF213* p.R4810K has not been identified in patients of European or Hispanic descent, other *RNF213* rare variants have been established to cause MMD in these other groups (12).

Recently, three consanguineous families with Moyamoya disease were reported with homozygous loss-of-function *GUCY1A3* mutations (13). All affected individuals had achalasia, a condition that prevents the esophageal sphincter from relaxing and leads to aperistalsis of the esophagus. A subset of affected individuals developed MMD. *GUCY1A3* encodes for the α 1 subunit of soluble guanylate cyclase (sGC), a ubiquitously expressed enzyme that is the only known receptor for nitric oxide (NO). sGC is a heterodimeric enzyme composed of one α and one β subunit, which are encoded by four genes in the human genome (α subunits by *GUCY1A3* and *GUCY1A2* and β subunits by *GUCY1B2* and *GUCY1B3*). Binding of NO to sGC increases its enzymatic activity, leading to

increased production of cGMP. The biological effects of cGMP are mediated by cGMP-dependent protein kinases I and II and cGMP-gated ion channels. These cGMP dependent kinases control the relaxation of smooth muscle cells (SMCs).

In this paper we report on two unrelated probands with compound heterozygous, loss-of-function mutations in *GUCY1A3* out of 96 unrelated MMD probands assessed for mutations. These findings demonstrate that *GUCY1A3* missense variants and variants that truncate the protein can cause autosomal recessive inheritance MMD and establishes the frequency of *GUCY1A3* mutations in a cohort of patients with MMD who are primarily of European descent.

MATERIALS AND METHODS

Study Population and Sample Collection

This study was approved by the Institutional Review Board at the University of Texas Health Science Center in Houston. Informed consent was obtained from all study participants. Over 140 families with one or more members affected with MMD were recruited or referred to an ongoing research study at the University of Texas Health Science Center at Houston (UTHealth) between 2003 and 2014. Individuals with Down syndrome, neurofibromatosis, sickle cell disease, disease-causing *RNF213* variants or other established genetic conditions predisposing to MMD were excluded from the study. *GUCY1A3* sequence results were obtained from 96 affected MMD probands. Disease presentation, confirmation of MMD by radiological findings and surgical history, clinical history, and demographics were abstracted from medical records and self-report. MMD was diagnosed based on magnetic resonance imaging (MRI), computed tomography (CT), or diagnostic angiogram findings demonstrating stenosis or occlusion of the terminal portion of the internal carotid artery with the formation of collateral vessels compensating for the arterial occlusion; patients with bilateral stenotic/occlusive internal carotid artery lesions without collateral formation were also included in the cohort. Patients in the cohort have either unilateral or bilateral disease. Complete family histories were obtained by a genetic counselor, including the diagnosis of MMD, stroke, coronary artery disease, and intracranial aneurysm, general medical history, and cardiovascular risk factors. Blood or saliva was collected from probands and family members, and DNA harvested using standard methods.

Exome and Sanger Sequencing

Genomic DNA from individuals with MMD and their family members was used for exome sequencing assay, and the exome sequences were captured by SeqCap EZ. Exome probes version 1.0 (Roche) Enriched libraries were then sequenced on an Illumina GAIIx using manufacturer protocols. Reads were mapped to the reference human genome (UCSC hg19) with BWA (Burrows-Wheeler Aligner) and variants called using SAMtools. Insertion-deletion (indel) variants affecting the coding sequence were identified after a Smith-Waterman realignment of the BWA calls. Single nucleotide variants (SNVs) and indels were filtered to $>8\times$ and quality >30 . Annotation of variants was performed using the SeattleSeq server (<http://gvs.gs.washington.edu/SeattleSeqAnnotation/>). Sanger DNA sequencing assay was performed by bi-directional direct sequencing of amplified genomic DNA fragments

with intron-based, exon-specific primers to validate exome sequencing results and sequence *GUCY1A3* in probands from unrelated families with MMD. *GUCY1A3* mutations were reported based on the RefSeq codes NM_000856.5.

Expression and Purification of sGC Enzyme

Site-directed mutagenesis was used to generate the *GUCY1A3* Cys517Tyr substitution in the coding region of the pVL- α_1 baculoviral transfer vector (14). This vector was used to generate the baculovirus expressing the α_1 Cys517 mutant sGC subunit. The wild type (WT) and the α_1 Cys517 enzymes were expressed in Sf9 cells and purified as described previously using the hexahistidine tag at the C-terminus of the α subunit (15). In short, 100,000 \times g supernatant of cell lysate was captured on a 30 ml column with DEAE-FF Sepharose (GE Lifescience) and, after extensive wash with 50 mM NaCl in 50 mM triethanolamine (TEA) pH 7.5, sGC-containing fractions were eluted with 350 mM NaCl. These sGC-positive fractions were loaded on a 20 ml Ni-agarose column (HisBind resin, Life Technologies). After a 30 mM imidazole wash, sGC enzyme was eluted with 175 mM imidazole. To remove the imidazole, the samples were captured on a 5 ml HiTrap DEAE-FF Sepharose column (GE Lifescience), washed and eluted by 300 mM NaCl. The sGC-containing fractions were concentrated on a YW-100 Centricon concentrator (Millipore). Preparations were at least 95% pure as determined by SDS-PAGE and Coomassie Blue staining.

Assay of sGC Activity

Enzyme activity of WT and α_1 Cys517 was assayed by the formation of [32 P] cGMP from α [32 P]GTP at 37°C as described previously (15). In short, the reaction was initiated by addition of 1 mM GTP to the enzyme in the buffer containing 25 mM TEA, pH 7.5, 1 mg/ml BSA, 1 mM cGMP, 3 mM MgCl₂, 0.05 mg/ml creatine phosphokinase and 5 mM creatine phosphate. To determine the GTP-K_m, the assay was performed at different concentrations of GTP (12.5 – 400 μ M range) for the indicated amount of time with and without 50 μ M DEA-NO. To determine the EC₅₀ for NO donor DEA-NO, different dilutions of DEA-NO prepared in 10 mM NaOH were added to the enzyme immediately before starting the reaction with 1 mM GTP/ α [32 P]GTP mix. In this case, the reaction was performed for 2 minutes at 37°C. The reactions were stopped by zinc acetate and processed as described previously (15).

UV-Vis spectra of the purified wild type $\alpha_1\beta_1$ sGC (WT) and mutant α Tyr517- β (mutant) sGC in 50 mM TEA pH 7.5, 200 mM NaCl and 1 mM DTT were recorded using a 8453 UV-VIS spectrophotometer (Agilent Technologies) in the regular mode.

Statistical Analysis

Nonlinear regression, calculation of EC₅₀ and statistical analysis was performed using GraphPad Prism 5.1 (GraphPad Software). One-way analysis of variance, followed by Turkey's post-hoc test was used for multiple comparisons. Two-way ANOVA followed by Bonferroni post-hoc test was used for comparison of the dose-response curves. P <0.05 was considered significant. Results are expressed as mean \pm SD. The EC₅₀ values are expressed as means with 95% confidence interval shown in brackets.

RESULTS

A cohort of MMD probands and their families has been recruited, and information on the affected probands is provided in Table I. To identify variants in genes that predispose to MMD, exome sequencing was pursued using DNA from 24 affected probands from unrelated families with MMD (12). Gene variants identified by whole exome sequencing that altered amino acid sequences of proteins, including non-synonymous, coding indel, frameshift, or splice site variants were further filtered based on the following minor allele frequencies (MAF) in the NHLBI Exome Sequencing Project (ESP) and modes of inheritance: 1) autosomal-dominant model: heterozygous variants with MAF more than 0.05% or heterozygous variants that were not present in all affected individuals from the same family were removed; 2) autosomal-recessive model: homozygous or potential compound heterozygous variants with MAF more than 0.5% were removed (16, 17). Among the candidate variants remaining, two nonsense variants, c.1258C>T (p.Arg420X) and c.1594G>T (p.Gly652X), in *GUCY1A3* (NM_000856.5) were identified in the proband of MMD041 family. Variant p.Arg420X has MAF 0.008% in the ESP database and is predicted to cause nonsense mediated mRNA decay. Variant p.Gly652X was not found in approximately 13000 chromosomes in the ESP database; this variant is not predicted to cause nonsense mediated mRNA decay. Family members are unavailable to confirm that these *GUCY1A3* rare variants are on separate alleles.

The *GUCY1A3* variants in the proband of MM149 were identified through clinical diagnostic testing (customized Blueprint Panel by the Baylor Medical Genetic Laboratories that included *RNF213*, *ACTA2*, *BRCC3*, *CBL*, *TIMP-2*, *MMP-2*, *MMP-3*, *SAMHD1*, *PSRC-1*, *TGFB1* and *PDGFRB*). Two variants were identified in *GUCY1A3*: c.334_335delGA (p.Glu112fs) and c.1550G>A (p.Cys517Tyr). Variants were identified using Next Generation Sequencing (NGS) and confirmed by Sanger sequencing. The unaffected father is heterozygous for the first variant; the mother is heterozygous for the second. The oldest, unaffected sibling has wild type alleles and the younger unaffected sibling is heterozygous for Cys517Tyr. The variant c334_335delGA (p.Glu112fs) has not been previously reported but is predicted to be pathogenic. The second variant, c.1550G>A (p.Cys517Tyr) is not found in the ESP and ExAC database. It was predicted to be damaging by Polyphen2, Sift, and Mutation Taster. The cysteine residue is a highly conserved amino acid with a PhyloP score of 6 and PhastCons score of 1. This variant is located at a Guanylate Cyclase Domain (473–690). Based on this information, it is likely to disrupt protein function. The domain organization of sGC heterodimer and the location of the identified mutations within sGC domains are depicted in Figure 1b.

Sanger sequencing using DNA from an additional 71 unrelated MMD probands identified no additional *GUCY1A3* rare variants. Thus, two probands with MMD disease out of a total of 96 unrelated probands had presumed biallelic rare variants in *GUCY1A3*.

Clinical Features of MMD Patients with Compound Heterozygous *GUCY1A3* Variants

The proband in family MM041 is a 28-year old Caucasian male born at 32 weeks via cesarean section, to non-consanguineous parents (Figure 1). He first presented at the 18 years of age with an ischemic stroke and visual field changes. Cerebral angiogram reveals

focal narrowing of the right internal carotid artery (ICA) prior to the cavernous carotid (Figure 2a). The distal portion of the ICA and its branches appear dilated. Collateral vessels at the skull base are apparent; however, classical moyamoya collaterals are not visualized (Figure 2b). Unlike the vasculature on the left side, the right-sided stenosis is more proximal to the terminal portion of the ICA with arterial dilatation distally. The left side presents with a more classic MMD appearance. The left ICA shows occlusion with filling of the anterior cerebral artery (ACA) and the middle cerebral artery (MCA) via typical basal moyamoya collateral vessels (Figure 2c–d). The left P1 segment is occluded, with multiple pial collaterals via the posterior cerebral artery (PCA) and its branches.

He underwent left encephalodural synangiosis shortly after his diagnosis. In the 10 years following his surgery, he reported recurrent TIAs, headaches, migraines, seizures, disorientation and memory problems. His medical history is also remarkable for achalasia diagnosed at the age of 4 years, gastroesophageal reflux disease and hypertension, along with asthma and cardiospasm. Patient reports that his achalasia was repaired surgically after diagnosis. He also had bilateral inguinal hernia repair. Family history was negative for MMD, stroke, seizure or migraine. This patient died in his sleep at the age of 28 years. No autopsy was done to determine the cause of death.

The proband in family MM149 is a 3 year old female born full term to non-consanguineous parents (Figure 1b). She presented with a severe right hemisphere stroke event at 20 months of age. MRA and cerebral angiogram revealed occlusion of the right terminal ICA artery and stenosis of the left supraclinoid and terminal ICA, consistent with MMD (Figure 3a and b, respectively). Right sided cerebral revascularization by dural inversion was performed. At 22 months, she presented with a second acute ischemic stroke. MRI imaging confirmed an acute left ACA and MCA infarct involving the cortex, white matter and deep grey matter; the mature right MCA cortical infarct was also evident. Patient underwent left-sided cerebral vascularization by dural inversion following the second cerebrovascular event. Follow up MRI imaging 6 months later shows evidence of bilateral MCA infarcts and generalized volume loss (Figure 3c).

The patient had a gastric tube inserted after her second stroke event due to dysphagia but achalasia was not diagnosed. Imaging of her renal arteries and aorta was ordered to further investigate the etiology of her hypertension at that time, which had been present since infancy, but this imaging showed no aortic coarctation or renal artery stenosis. At the age 3 years, she was found to have enlargement of her ascending aorta (diameter 1.8 cm; Z score 2.3) with a normal aortic root. Prior to her stroke she met all of her developmental milestones. Physical exam by a geneticist noted no dysmorphic features or birth defects.

Family history is negative for MMD. Maternal grandfather suffered a stroke at the age of 50 years. Father has a history of hypertension, onset in his mid 20's, with poor response to medication. Paternal family history is significant for hypertension and strokes in paternal great-grandparents in their 80's.

Biochemical Characterization of the *GUCY1A3* variant Cys517Tyr

To determine if the *GUCY1A3*Tyr517 in the α_1 subunit affects the biochemical properties of sGC, plasmids with either the α_1 wildtype or the Tyr517 subunits, along with the wildtype β_1 subunit, were co-expressed in a Sf9 cells using baculovirus expression system. The primary function of sGC is to serve as an effective receptor for NO and to amplify this signal by generating the secondary messenger, cGMP. Therefore, we compared the activity of the WT $\alpha_1 \beta_1$ sGC with the α_1 Tyr517 β_1 mutant sGC in the absence of NO and in the presence of different concentrations of the NO donor DEA-NO. As shown in Figure 4a and Table 2, the α_1 Tyr517 β_1 enzyme exhibited diminished cGMP forming activity under basal conditions and a more pronounced impairment under NO-induced conditions. As expected, the WT sGC demonstrated a robust 193 ± 18 fold activation by saturating concentrations of NO, while α_1 Tyr517 β_1 exhibited a more moderate response with a 114 ± 5 fold activation. The maximal activity was also significantly different (9.02 ± 0.32 vs 3.01 ± 0.12 μ mole cGMP/min/mg). Despite this significant difference in the cGMP-forming activity between the two enzymes, we determined that EC_{50} for DEA-NO was almost identical. The estimated DEA-NO EC_{50} for the wild type sGC was 28 [22–35] nM vs. 25 [15–45] nM for α_1 Tyr517. Consistent with this observation, purified $\alpha_1\beta_1$ and α_1 Tyr517 β_1 enzymes had the same ultraviolet-visible spectra of their heme moiety, with a maximal Soret band at 432 nm and a broad α/β band in the 520–590 nm region.

Since these analyses showed that the catalytic function of sGC is primarily affected with the C517Y variant, we compared the K_m for the substrate GTP between the $\alpha_1\beta_1$ and α_1 Tyr517 β_1 enzymes. As presented in Table 2, the GTP- K_m values for α_1 Tyr517 β_1 was larger in both for basal and NO-induced states. Consistent with previous studies, the GTP- K_m decreases upon activation with NO, but this decrease was more pronounced for $\alpha_1\beta_1$ than for α_1 Tyr517 β_1 . Taken together, these biochemical studies indicate that the *GUCY1A3* Cys517Tyr variant should result in a significantly blunted response to NO signaling, due to impaired function of the catalytic region of α_1 Tyr517 β_1 .

DISCUSSION

Our study indicates that compound heterozygous mutations in *GUCY1A3* cause MMD associated with achalasia and hypertension. In our cohort, *GUCY1A3* mutations were found in two out of 96 unrelated probands, indicating that *GUCY1A3* mutations are a rare cause of MMD. The initial three unrelated families with *GUCY1A3* mutations had homozygous loss-of-function mutations that were shown to produce no α_1 subunit of sGC based on assessment of the affected patients' platelets. The cases reported here differ from the previously reported mutations in that the MMD patients have compound heterozygous rare variants in *GUCY1A3*. In both cases, one allele is a nonsense or frameshift mutation predicted to lead to nonsense mediated decay with no protein produced. The second allele from both patients is predicted to produce a mutant protein, specifically a truncated protein in MM041 and a protein with a missense mutation in MM149. In MM041 case, a truncated protein lacking the last 33 residues of the C-terminal catalytic region of the α_1 subunit is expected. Based on the recently reconstructed X-ray structure of the catalytic region of sGC (18), these residues are essential for the proper folding of the distal region of the functional

catalytic domain. Recent studies demonstrated that the sGC enzyme with perturbation in this distal region has a strongly impaired cGMP synthesis (19). Similar impairment of cGMP synthesis is expected for the p.Gly652X allele. In MM149 case, a protein with a missense Cys→Tyr substitution in position 517 of the $\alpha 1$ subunit is generated. Biochemical analysis presented in current studies confirmed that the missense mutation, *GUCYIA3* Cys517Tyr, leads to a significantly blunted response in NO signaling and decreased cGMP production. Taking into consideration the K_m and V_{max} values determined in this study (Table 2) and the average intracellular GTP concentration of $\sim 100 \mu\text{M}$ (20, 21), it is easy to predict that even with saturating concentrations of NO the rate of NO-dependent synthesis of cGMP in cell with *GUCYIA3* Cys517Tyr allele will be at least 5 times lower. These biochemical data are consistent with previously published observation on rat $\alpha 1\beta 1$ sGC containing nitrosylated Cys516 (22). It has been reported that nitrosylation of Cys516 in rats, which is homologous to the Cys517 in humans, results in desensitization of sGC to NO activation. It appears that the polar -OH moiety introduced by the α Cys517Tyr has the same effect on sGC enzymatic function as the introduction of the polar NO moiety in the $\alpha 516\text{Cys-NO}$ enzyme.

The presentation of affected individuals in the previously reported three families with *GUCYIA3* mutations was characterized by the onset of achalasia under the age of 15 months and reduced penetrance of MMD with an onset under 3 years of age (13). All individuals underwent Heller myotomy, a laparoscopic surgical intervention, for their achalasia. Of note, the lack of relaxation in the esophageal sphincter suggests that achalasia is caused by an interruption in the nitric oxide signaling pathway. In contrast, the affected proband in family MM041 was diagnosed with achalasia at the age of 4 years and MMD at 18 years of age, indicating an older age of presentation of both complications. The affected proband of family MM149 presented with MMD at 20 months of age, an early onset similar to the previously reported cases and has not been diagnosed with achalasia. Thus, presentation with MMD in the absence of achalasia occurs with *GUCYIA3* mutations. It is important to note that patients reported to date with complete medical records all have hypertension, and hypertension was already present in the 20 month old child reported in this study. She also has mild enlargement of her ascending aorta, which may be due to the chronic hypertension or the underlying mutation.

Unlike patients with *ACTA2* p.Arg179 mutations, a thorough review of imaging studies, including cerebral angiogram, MRI and MRA studies, has shown no radiological signature that can distinguish MMD in patients with *GUCYIA3* mutations. Several of the patients reported have been described with the characteristic arteriopathy of MMD; however, some cases have atypical features such as the dilatation seen in MM041, indicating that the phenotype may be broad. Although mutations in this gene are a rare cause of MMD, it should not be excluded as a possible etiology during evaluation for moyamoya disease, particularly in the presence of hypertension and/or achalasia.

GUCYIA3 encodes the $\alpha 1$ subunit of sGC, which pairs with the $\beta 1$ subunit encoded by *GUCYIB3* to make the heterodimeric enzyme subunit. The isoform is abundantly expressed in vascular SMCs, where it regulates SMC relaxation and vascular tone. Although the sGC $\alpha 1\beta 1$ heterodimer is the most abundant sGC isoform in the vasculature, low levels of

cGMP, generated by sGC $\alpha_2\beta_1$, are sufficient to mediate many of NO's cardiovascular effects in mice (23). Despite some compensation by sGC $\alpha_2\beta_1$, male mice, but not female mice, deficient for the α_1 subunit sGC develop hypertension (18). Therefore, the consistent complication of hypertension in patients, both males and females, with biallelic *GUCY1A3* mutations may be due to the decreased relaxation of the SMCs in the vasculature.

The etiology of the predisposition for MMD is less clear. It is notable that the loss of expression of one allele of *GUCY1A3*, in combination with a missense variant in *CCT7* (a gene that encodes a protein that stabilizes sGC), was found to increase the risk for myocardial infarct in a large family (24). Additionally, two genome wide association studies identified a common variant in *GUCY1A3* associated with myocardial infarct or coronary artery disease (25, 26). Thus, there is accumulating evidence that variants in *GUCY1A3* cause occlusive vascular disease, including MMD and coronary artery disease, increasing the relevance of defining the molecular pathways leading to these occlusive vascular diseases. It has already been demonstrated that loss of the α_1 subunit of sGC in mice leads to enhanced thrombus formation; therefore the occlusive arterial lesions in patients with *GUCY1A3* mutations could be due to increased thrombus formation (24). Alternatively, decreased sGC activity in vascular SMCs could increase the proliferation of these cells, leading to increased neointimal lesions. An altered hyperplastic SMC phenotype is hypothesized to lead to MMD in patients with *NF1* and *ACTA2* mutations (27, 28). Increased proliferation as a cause of the MMD is also supported by the marked neointimal proliferation as the cause of the cerebrovascular occlusions reported in MMD patients (29). Stimulators of sGC have been shown to reduce vascular SMC proliferation, suggesting that loss of sGC would increase SMC proliferation (30). Delineating these possible molecular pathways leading to arterial occlusion and MMD is an important step towards developing therapeutic strategies to prevent this cerebrovascular disease.

When determining the genetic etiology in patients with MMD, an initial assessment is necessary to rule out syndromic forms, such as Down syndrome, neurofibromatosis (*NF1*), sickle cell anemia, primordial dwarfism (*PCNT*) or Alagille syndrome (*JAG1*). In the absence of findings that suggest one of these conditions, panel testing should be considered. With the addition of *GUCY1A3*, there are approximately 5 genes that have been found to have disease-causing variants leading to moyamoya disease. At this time, a panel should include *RNF213*, particularly if the patient is of Asian descent (Japanese, Chinese, Indian, Bangladeshi, Pakastani), as the disease causing p.R4810K variant is found in these populations, *BRCC3* (X-linked inheritance) (5), *ACTA2*, and *SAMHD1* (31). Going forward, whole exome sequencing may be a valid initial approach to identify an underlying genetic cause of MMD. The exome data can be reviewed for variants in the known genes for MMD, and several commercial labs offer the opportunity to data-mine the exome information several years after the original report. With the expansion of the understanding of the genes predisposing to MMD, a patient's exome data can be mined for rare variants in newly identified genes, rather than sequencing each individual gene as it is identified.

In summary, although *GUCY1A3* mutations are a rare cause of MMD, the presence of achalasia or hypertension should also raise the suspicion of mutations in this gene. The presence of variability and overlap in presentation of intracranial arteriopathy suggests that

when exploring the genetic basis of MMD, testing a panel of genes associated with MMD that includes *GUCY1A3* should be considered in individuals with MMD.

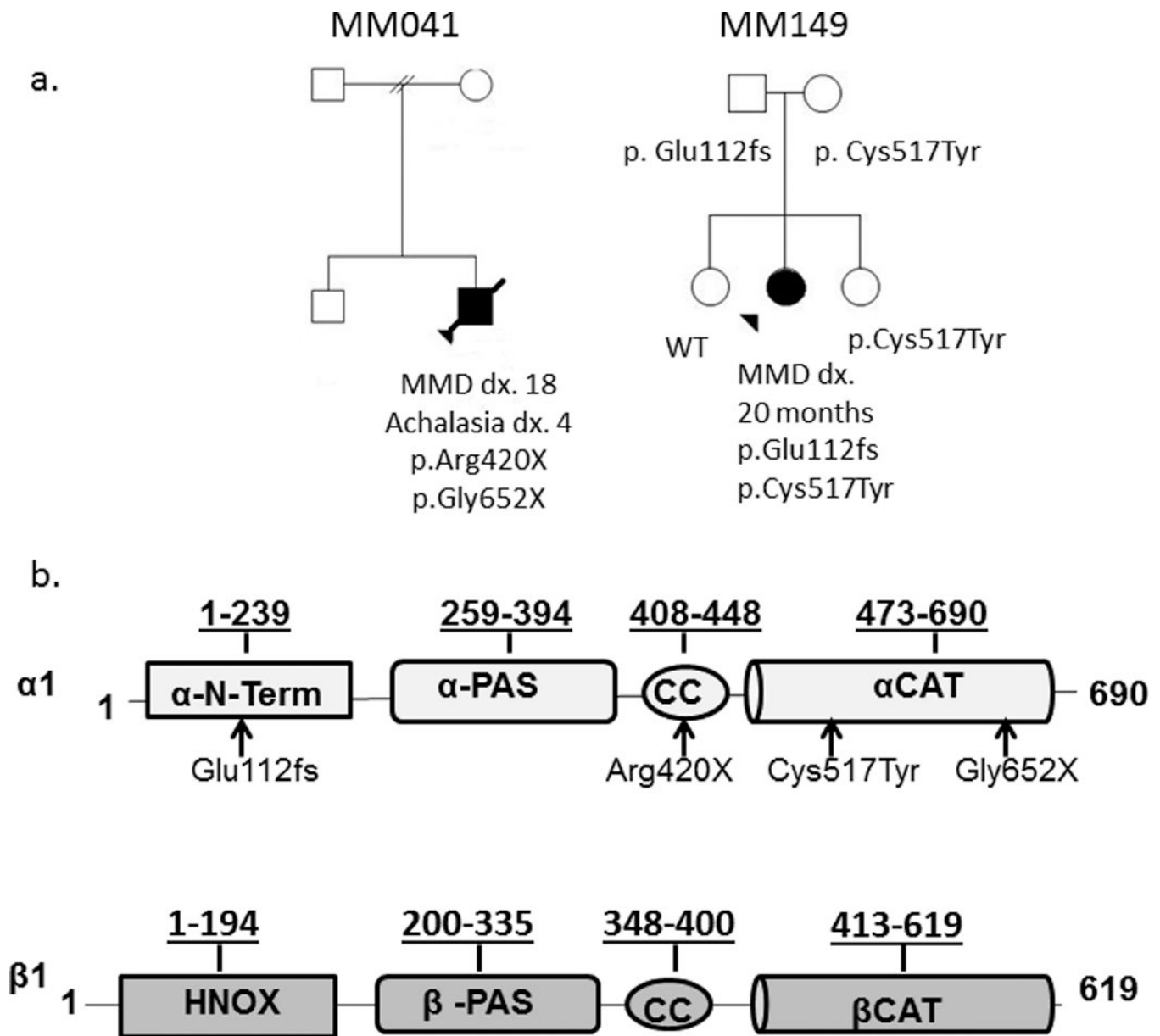
Acknowledgments

We are grateful to the patients and families for their participation in this research. This work was supported by RO1 HL62594 (D.M.M) from the National Institutes of Health (NIH) and funds from the Vivian L. Smith Foundation (D.M.M). NIH funding was also provided to the University of Washington Center for Mendelian Genomics (1U54HG006493) and to the University of Texas Health Science Center at Houston (UL1 RR024148) and American Heart Association Grant-in-Aid 15GRNT25700101 (E.M).

References

1. Scott RM, Smith ER. Moyamoya disease and moyamoya syndrome. *N Engl J Med.* 2009; 360(12): 1226–1237. [PubMed: 19297575]
2. Woolfenden AR, Albers GW, Steinberg GK, et al. Moyamoya syndrome in children with Alagille syndrome: additional evidence of a vasculopathy. *Pediatrics.* 1999; 103(2):505–508. [PubMed: 9925853]
3. Rea D, Brandsema JF, Armstrong D, et al. Cerebral arteriopathy in children with neurofibromatosis type 1. *Pediatrics.* 2009; 124(3):e476–e483. [PubMed: 19706560]
4. Rosser TL, Vezina G, Packer RJ. Cerebrovascular abnormalities in a population of children with neurofibromatosis type 1. *Neurology.* 2005; 64(3):553–555. [PubMed: 15699396]
5. Miskinyte S, Butler MG, Herve D, et al. Loss of BRCC3 deubiquitinating enzyme leads to abnormal angiogenesis and is associated with syndromic moyamoya. *Am J Hum Genet.* 2011; 88(6):718–728. [PubMed: 21596366]
6. Mineharu Y, Takenaka K, Yamakawa H, et al. Inheritance pattern of familial moyamoya disease: autosomal dominant mode and genomic imprinting. *J Neurol Neurosurg Psychiatry.* 2006; 77(9): 1025–1029. [PubMed: 16788009]
7. Scott RM, Smith JL, Robertson RL, et al. Long-term outcome in children with moyamoya syndrome after cranial revascularization by pial synangiosis. *J Neurosurg.* 2004; 100(2 Suppl Pediatrics):142–149. [PubMed: 14758941]
8. Munot P, Saunders DE, Milewicz DM, et al. A novel distinctive cerebrovascular phenotype is associated with heterozygous Arg179 ACTA2 mutations. *Brain.* 2012; 135(Pt 8):2506–2514. [PubMed: 22831780]
9. Guo DC, Papke CL, Tran-Fadulu V, et al. Mutations in smooth muscle alpha-actin (ACTA2) cause coronary artery disease, stroke, and moyamoya disease, along with thoracic aortic disease. *Am J Hum Genet.* 2009; 84(5):617–627. [PubMed: 19409525]
10. Kamada F, Aoki Y, Narisawa A, et al. A genome-wide association study identifies RNF213 as the first Moyamoya disease gene. *J Hum Genet.* 2011; 56(1):34–40. [PubMed: 21048783]
11. Liu W, Morito D, Takashima S, et al. Identification of RNF213 as a susceptibility gene for moyamoya disease and its possible role in vascular development. *PLoS ONE.* 2011; 6(7):e22542. [PubMed: 21799892]
12. Cecchi AC, Guo D, Ren Z, et al. RNF213 rare variants in an ethnically diverse population with Moyamoya disease. *Stroke.* 2014; 45(11):3200–3207. [PubMed: 25278557]
13. Herve D, Philippi A, Belbouab R, et al. Loss of alpha1beta1 soluble guanylate cyclase, the major nitric oxide receptor, leads to moyamoya and achalasia. *Am J Hum Genet.* 2014; 94(3):385–394. [PubMed: 24581742]
14. Lee DF, Chen CC, Hsu TA, et al. A baculovirus superinfection system: efficient vehicle for gene transfer into *Drosophila* S2 cells. *J Virol.* 2000; 74(24):11873–11880. [PubMed: 11090187]
15. Martin E, Sharina I, Kots A, et al. A constitutively activated mutant of human soluble guanylyl cyclase (sGC): implication for the mechanism of sGC activation. *Proc Natl Acad Sci U S A.* 2003; 100(16):9208–9213. [PubMed: 12883009]

16. Boileau C, Guo DC, Hanna N, et al. TGFB2 mutations cause familial thoracic aortic aneurysms and dissections associated with mild systemic features of Marfan syndrome. *Nat Genet.* 2012; 44(8):916–921. [PubMed: 22772371]
17. Shearer AE, Eppsteiner RW, Booth KT, et al. Utilizing ethnic-specific differences in minor allele frequency to recategorize reported pathogenic deafness variants. *Am J Hum Genet.* 2014; 95(4): 445–453. [PubMed: 25262649]
18. Seeger F, Quintyn R, Tanimoto A, et al. Interfacial residues promote an optimal alignment of the catalytic center in human soluble guanylate cyclase: heterodimerization is required but not sufficient for activity. *Biochemistry.* 2014; 53(13):2153–2165. [PubMed: 24669844]
19. Martin E, Golunski E, Laing ST, et al. Alternative splicing impairs soluble guanylyl cyclase function in aortic aneurysm. *Am J Physiol Heart Circ Physiol.* 2014; 307(11):H1565–H1575. [PubMed: 25239802]
20. Hatakeyama K, Harada T, Kagamiyama H. IMP dehydrogenase inhibitors reduce intracellular tetrahydrobiopterin levels through reduction of intracellular GTP levels. Indications of the regulation of GTP cyclohydrolase I activity by restriction of GTP availability in the cells. *J Biol Chem.* 1992; 267(29):20734–20739. [PubMed: 1356983]
21. Otero AD. Transphosphorylation and G protein activation. *Biochem Pharmacol.* 1990; 39(9):1399–1404. [PubMed: 2159303]
22. Crassous PA, Couloubaly S, Huang C, et al. Soluble guanylyl cyclase is a target of angiotensin II-induced nitrosative stress in a hypertensive rat model. *Am J Physiol Heart Circ Physiol.* 2012; 303(5):H597–H604. [PubMed: 22730391]
23. Mergia E, Friebe A, Dangel O, et al. Spare guanylyl cyclase NO receptors ensure high NO sensitivity in the vascular system. *J Clin Invest.* 2006; 116(6):1731–1737. [PubMed: 16614755]
24. Erdmann J, Stark K, Esslinger UB, et al. Dysfunctional nitric oxide signalling increases risk of myocardial infarction. *Nature.* 2013; 504(7480):432–436. [PubMed: 24213632]
25. Deloukas P, Kanoni S, Willenborg C, et al. Large-scale association analysis identifies new risk loci for coronary artery disease. *Nat Genet.* 2013; 45(1):25–33. [PubMed: 23202125]
26. Luo X, Xiao Y, Song F, et al. Increased plasma S-adenosyl-homocysteine levels induce the proliferation and migration of VSMCs through an oxidative stress-ERK1/2 pathway in apoE(–/–) mice. *Cardiovasc Res.* 2012; 95(2):241–250. [PubMed: 22492673]
27. Xu J, Ismat FA, Wang T, et al. NF1 regulates a Ras-dependent vascular smooth muscle proliferative injury response. *Circulation.* 2007; 116(19):2148–2156. [PubMed: 17967772]
28. Papke CL, Cao J, Kwartler CS, et al. Smooth muscle hyperplasia due to loss of smooth muscle alpha-actin is driven by activation of focal adhesion kinase, altered p53 localization and increased levels of platelet-derived growth factor receptor-beta. *Hum Mol Genet.* 2013
29. Reid AJ, Bhattacharjee MB, Regalado ES, et al. Diffuse and uncontrolled vascular smooth muscle cell proliferation in rapidly progressing pediatric moyamoya disease. *J Neurosurg Pediatr.* 2010; 6(3):244–249. [PubMed: 20809708]
30. Joshi CN, Martin DN, Fox JC, et al. The soluble guanylate cyclase stimulator BAY 41-2272 inhibits vascular smooth muscle growth through the cAMP-dependent protein kinase and cGMP-dependent protein kinase pathways. *J Pharmacol Exp Ther.* 2011; 339(2):394–402. [PubMed: 21825001]
31. Xin B, Jones S, Puffenberger EG, et al. Homozygous mutation in SAMHD1 gene causes cerebral vasculopathy and early onset stroke. *Proc Natl Acad Sci U S A.* 2011; 108(13):5372–5377. [PubMed: 21402907]

**Figure 1.**

(a) Pedigrees of the families MM041 and MM149. Samples from additional family members were not available to determine segregation of the *GUCY1A3* variants in family MM041. Segregation of the *GUCY1A3* rare variants in family MM149 show that the unaffected parents and unaffected sibling are heterozygous for a rare variant, the oldest siblings is wild type, and the affected proband has inherited both rare variants. Circles represent women; squares represent men. Pedigree symbols filled in black indicate the individual is affected, and a line through the symbol indicates the individual has died. **(b) Domain organization of sGC $\alpha 1$ and $\beta 1$ splice subunits.** HNOX – domain binding heme/NO/oxygen; PAS - Per/Arnt/Sim domain; CC- coiled coil domain; CAT – catalytic domain. The underlined numbers above bars are domain boundaries. The arrows indicate the positions of identified mutation.

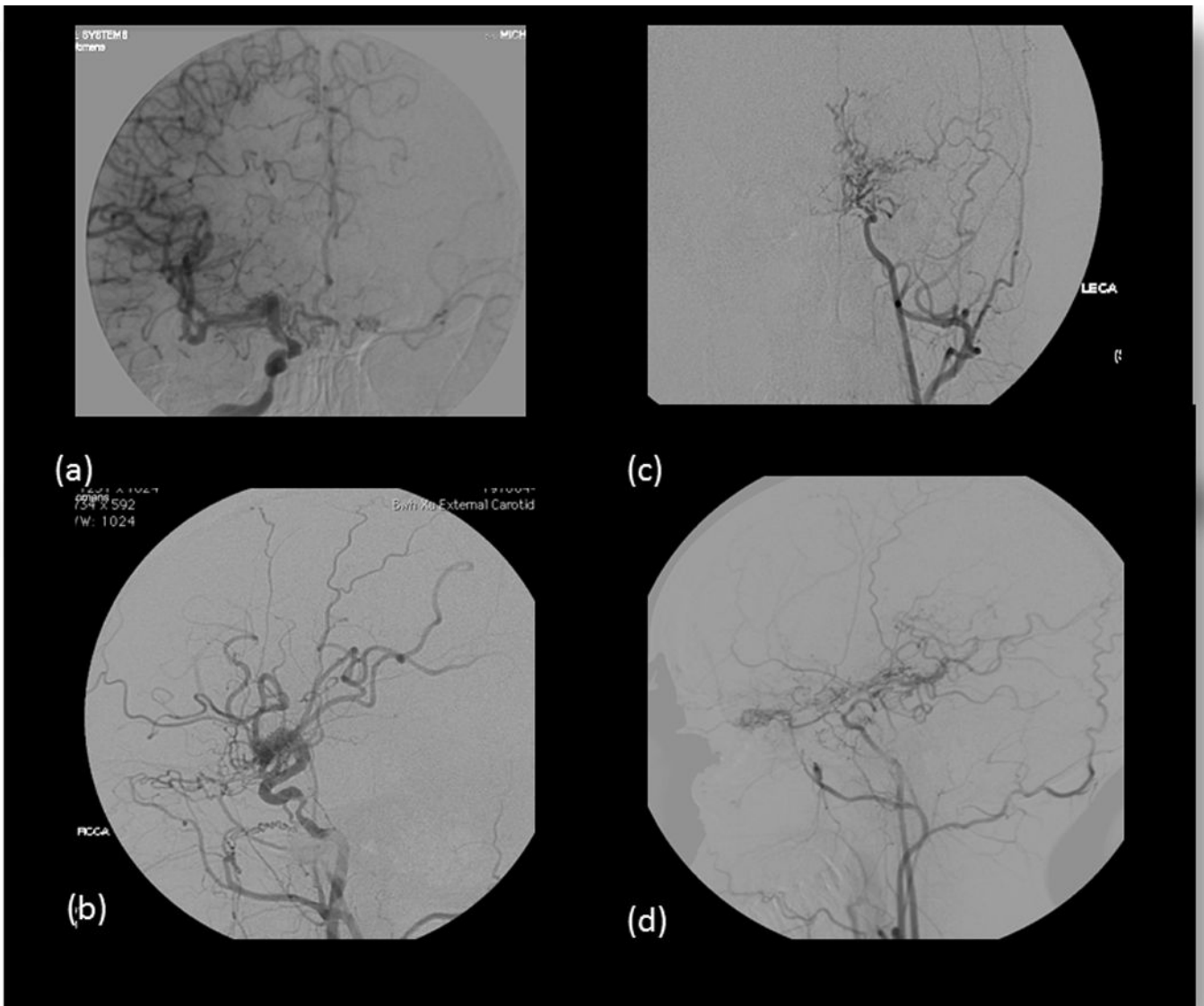


Figure 2.

Cerebral angiogram for proband of MM041. AP view of (a) R internal carotid artery angiogram. On the right, there is focal narrowing of the ICA just proximal to its cavernous segment. The more distal ICA and its branches appear dilated, as apparent on the lateral projection (b) Basal "moyamoya" collaterals are not seen on the right, although other collateral vessels are apparent at the skull base. (c) AP and (d) lateral views of left internal carotid artery angiogram showing occlusion of the ICA distal to the ophthalmic artery with typical basal "moyamoya" collaterals. The left P1 segment was occluded; there were multiple pial collaterals from the posterior circulation supplying both hemispheres.

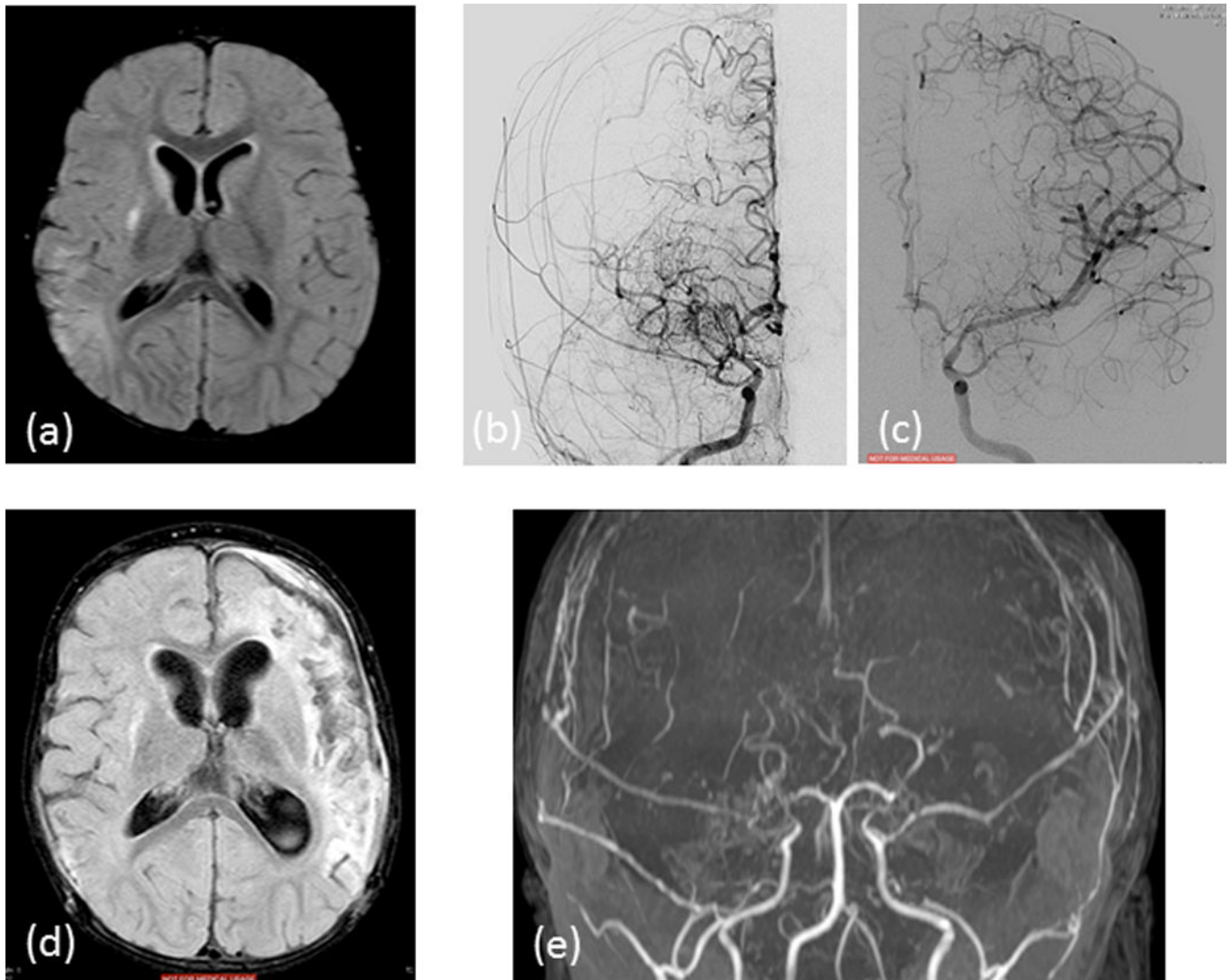
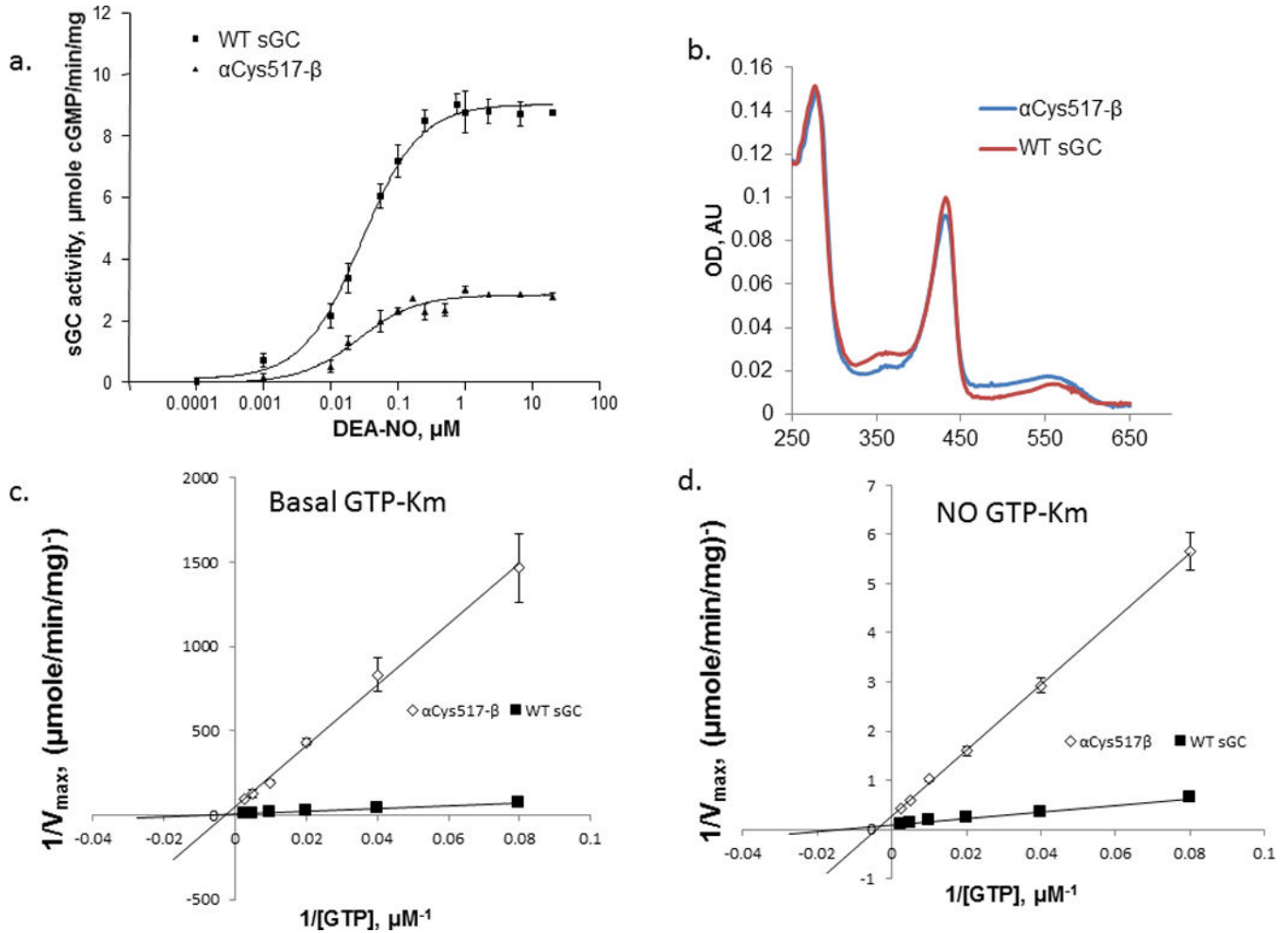


Figure 3.

Images from proband of MM149, a 20 month old child at the time of initial presentation. (a) AP view of right common carotid angiogram shows occlusion of the MCA with some distal filling via multiple basal collaterals; the proximal ACA is narrow but there is good distal filling. (b) AP view of left internal carotid angiogram shows mild narrowing of the terminal ICA and proximal ACA, without basal collaterals and good distal filling. The posterior circulation is normal and provides collateral supply to the hemispheres. She had an acute, left MCA territory infarct 2 months later. Six months from initial presentation, (c) axial FLAIR imaging shows established bilateral MCA territory infarcts and generalized volume loss. On time of flight MRA of the circle of Willis (d) there is bilateral progression of the occlusive arteriopathy. The child has had bilateral surgical revascularization.

**Figure 4.**

Impaired activation of α_1 Tyr517- β_1 sGC. (a): The activity of the wild type $\alpha_1\beta_1$ in the presence of the donor DEA-NO, as determined by a 2 minute assay at 37°C. Shown data are mean \pm SD from three independent measurements performed in triplicates using two different enzyme preparations. $p < 0.001$ (two-way ANOVA). (b): The UV-Vis spectrum of 0.1 mg/ml purified wild type $\alpha_1\beta_1$ sGC and mutant α_1 Tyr517 β_1 sGC in 50 mM TEA and 200 mM NaCl. (c–d): Determination of GTP- K_m for the wild type $\alpha_1\beta_1$ sGC and mutant α_1 Tyr517- β_1 sGC in the absence (c) and presence (d) of 50 μM DEA-NO. Data (mean \pm SD) are based on three independent measurements performed in triplicates using two different enzyme preparations.

Table 1

Demographic and Clinical Information on the Moyamoya Disease Cohort

Variable		Total = 96
Average age at diagnosis (Range)		27.7 years (9 months–58 years)
Sex		
	Female	74 (76%)
	Male	22 (24%)
Ethnicity		
	European descent	71 (73%)
	African American	7 (7%)
	Hispanic/Latino	3 (3%)
	Asian	5 (5%)
	Multiple Ethnicities	3 (3%)
	Not Specified	7 (8%)
Laterality of MMD		
	Bilateral	60 (62%)
	Unilateral	28 (29%)
	Unknown	8 (9%)

Table 2

Characterization of the wild type and mutant (α_1 Cys517Tyr β_1) soluble guanylate cyclase.

	Wild type $\alpha_1\beta_1$ sGC	Mutant α_1 Tyr517 β_1 sGC
UV-Vis bands: α and β bands γ (Soret) band	Broad band at 520–620 nm 432 nm maximum	Broad band at 520–620 nm 432 nm maximum
Basal cGMP forming activity	0.047 ± 0.01 μ mole cGMP/min/mg	0.026 ± 0.001 μ mole cGMP/min/mg
Maximal NO-induced activity	9.02 ± 0.32 μ mole cGMP/min/mg	3.01 ± 0.12 μ mole cGMP/min/mg
Fold activation	193 ± 18	114 ± 5
GTP-K_m: Basal NO-induced	223.2 ± 18.2 μ M 74.6 ± 6.1 μ M	365.8 ± 68.1 μ M 195.6 ± 9.3 μ M

Author Manuscript

Author Manuscript

Author Manuscript

Author Manuscript